Numerical Simulation of Polymer Phase Separation on a Patterned Substrate with Nano Features

Yingrui Shang*, David Kazmer**, Ming Wei, Joey Mead, and Carol Barry
Department of Plastics Engineering, University of Massachusetts at Lowell
*yingrui_shang@student.uml.edu
**david_kazmer@uml.edu

ABSTRACT

Phase separation of an asymmetric immiscible binary polymer system in an elastic field with the existence of a patterned substrate was numerically studied in 2D and 3D. An unconditionally stable method for time marching the Cahn-Hilliard equation was employed in the numerical simulation. Compared to the conventional interface tracing mechanism, this diffusion controlled system is characterized by a thick interface with a composition gradient. The evolution mechanisms were studied. The evolution of the characteristic length, $R(t)$, of the phase separation morphology patterns was measured with the Fast Fourier Transform method. The results indicated $R(t)^{1/3}$ increases linearly with time. The influence of the material composition, the attraction factor on the template, and the gradient energy coefficient between the two polymers on the result patterns were also observed in this study. Qualitative and quantitative correspondence can be observed between the numerical results and the experiment results.

Keywords: spinodal decomposition, numerical simulation, patterned substrate, discrete cosine transform

1 FUNDAMENTALS

The thermodynamic behavior of a spinodal decomposition of a blend can be described by Cahn-Hilliard Equation [1], the free energy, F, with the consideration of a surface energy on the substrate in our study, for a binary system can be written as:

$$F(C)=\int_V \{f+f_e+\kappa(\nabla C)^2\}dV+\int_S f_S(C,\mathbf{r})dS \qquad 1$$

where C is the mole fraction of one polymer component, f is the local free-energy density of homogeneous material, f_e is the elastic energy density, and κ is the gradient energy coefficient. Thus the term $\kappa(\nabla C)^2$ is the additional free energy density if the material is in a composition gradient.

The free energy variation on the heterogeneously functionalized substrate is simulated by a free energy term, f_s, which is a function of the composition and the coordinates, $\mathbf{r}$, as well. The surface free energy is added to the total free energy on the surface of the substrate.

The evolution of the composition can be written as the function of local composition:

$$\frac{dC}{dt}=\nabla^2\cdot\left[M\left(\frac{\partial f}{\partial C}+\frac{\partial f_e}{\partial C}-\kappa\nabla^2 C\right)\right] \qquad 2$$

The Flory-Huggins type of free energy [2] is used to model the bulk free energy density

$$f=\frac{RT}{v_{site}}\left(\frac{C_A}{m_A}\ln C_A+\frac{C_B}{m_B}\ln C_B+\chi_{AB}C_AC_B\right) \qquad 3$$

where C_i is the volume fraction of component i, m_i is the degree of polymerization of component i, T is the temperature in K, R is the ideal gas constant, χ_{AB} is the Flory-Huggins interaction parameters between two components, which is dependent on temperature, and v_{site} is the molar volume of the reference site in the Flory-Huggins lattice model.

The elasticity is assumed isotropic in the domain. According to the Vegard's law [3], the stress-free strain is isotropic and depends linearly on the composition:

$$e_{ij}^0=\eta(C-C_0)\delta_{ij} \qquad 4$$

where e_{ij}^0 is the stress-free strain, c_0 is the average composition of the domain, δ_{ij} is the Kronecker delta function, and η is the compositional expansion coefficient which is expected to be independent of the composition and the composition gradient [4].

According to the linear elasticity, the stress, σ_{ij} is linear with the change of the strain by Hook's law:

$$\sigma_{ij}=c_{ijkl}\left(e_{kl}-e_{kl}^0\right) \qquad 5$$

where c_{ijkl} represents the isothermal elastic tensor, which is independent of position and composition. The elastic energy then can be expressed as follows, with no external anisotropic elastic applied,

$$f_e=\frac{1}{2}c_{ijkl}\left(e_{ij}-e_{ij}^0\right)\left(e_{kl}-e_{kl}^0\right) \qquad 6$$

The total strain can be evaluated by the local displacement, $\mathbf{u}$ [5].

$$e_{ij}=\frac{1}{2}\left(\frac{\partial u_i}{\partial r_j}+\frac{\partial u_j}{\partial r_i}\right) \qquad 7$$

The displacement of the reference lattice is then solved by the elastic equilibrium. Given the fast relaxation time compared to the rate of morphology evolution, it can be assumed that the system is in elastic equilibrium [6]:

$$\frac{\partial \sigma_{ij}}{\partial r_j} = 0 \qquad 8$$

2 NUMERICAL METHODS

The Cahn-Hilliard equation is known for its difficulty to solve due to its non-linearity and the bihamonic term. The cosine transform method is applied to the spatial discretization:

$$\frac{d\hat{C}}{dt} = M\lambda\left(\left\{\frac{\partial f}{\partial C} + \frac{\partial f_e}{\partial C}\right\} - \kappa\lambda\hat{C}\right) \qquad 9$$

where $\hat{C}$ and $\left\{\frac{\partial f}{\partial C} + \frac{\partial f_S}{\partial C}\right\}$ represent the cosine transform of the respective terms in Equation 4. λ is the approximation of discrete Laplacian operator in the transform space [7]:

$$\lambda(\mathbf{k}) = \frac{2\sum_i \cos(2\pi k_i) - \sum_i 2}{(\Delta x)^2} \qquad 10$$

The vector **k** denotes the discretisized spatial element position in all dimensions. Numerically, $k_i = n_i/N_i$, where n_i is the element in the ith dimension and N_i represents the number of elements in the ith dimension. Δx is the spatial step in the numerical modeling.

By this means, the partial differential equation is transformed into an ordinary differential equation in the discrete cosine space. A semi-implicit method is used to trade off the stability, computing time and accuracy [8, 9]. The linear fourth-order operators can be treated implicitly and the nonlinear terms can be treated explicitly. The resulting first-order semi-implicit scheme is:

$$(1 + M\Delta t\kappa\lambda)\hat{C}^{n+1} = \hat{C}^n - M\Delta t\lambda\left\{\frac{\Delta f(C^n)}{\Delta C} + \frac{\Delta f_e(C^n)}{\Delta C}\right\} \qquad 11$$

A second-order Adams-Bashforth method [10] was also used for the explicit treatment of the nonlinear term after the first time step,

$$\begin{aligned}(3 + 2M\Delta t\kappa\lambda^2)\hat{C}^{n+1} &= 4\hat{C}^n - \hat{C}^{n-1} \\ &+ 2M\Delta t\lambda\left(\begin{array}{l} 2\left\{\frac{\partial f(C^n)}{\partial C} + \frac{\partial f_e(C^n)}{\partial C}\right\} \\ -\left\{\frac{\partial f(C^{n-1})}{\partial C} + \frac{\partial f_e(C^{n-1})}{\partial C}\right\}\end{array}\right)\end{aligned} \qquad 12$$

The parameters are selected according to the corresponding experiment conditions and the literature. The temperature is 363K (90^0C). The degree of polymerization of polymer A and B are 447 and 915. The interaction parameter, χ_{AB}, in the Flory-Huggins type of free energy is evaluated as 0.117 with an empirical function by Kressler et. al. [11]. The gradient energy coefficient, κ, is selected as 6.9e-11J/m [12] for a generic polymer material. The diffusivity, D=1e-20m^2/s, is chosen as a typical value for polymers. The mobility of the system then can be evaluated.

In the elastic model, the reference composition is chosen according to the initial condition. The compositional expansion coefficient is chosen as η=0.02 [12].

The surface energy is simulated as linear to the local composition [13].

$$f_S(C, \mathbf{r}) = s_0(\mathbf{r}) + s_1(\mathbf{r})(C - C_{ref}) \qquad 13$$

where $s_0(\mathbf{r})$ and $s_1(\mathbf{r})$ are surface attraction parameters that represent the functionalization of the substrate, and C_{ref} is the reference composition. For non-dimensionalization, C_{ref} and $s_0(\mathbf{r})$ are chosen to be 0. The functionalized substrate energy factor $s_1(\mathbf{r})$ is alternating across the x direction of the substrate in an effort to develop a corresponding alternating strip patterns in the self-assembling polymer near the substrate.

3 RESULTS AND DISCUSSION

The characteristic length is then measured with respect to time. In the numerical modeling, the domain growth is studied by evaluating the pair-correlation functions g_i, where the subscript i and j represents the directions in the domain [14].

$$g_i(d,t) = \frac{1}{N_j}\sum_{k_j=1}^{N_j} g_{i,k_j}(d,t) \qquad 14$$

where $g_{i,ki}$ is defined as

$$g_{i,k_j}(d,t) = \left\langle \psi\left(\mathbf{k} = (k_i, k_j), t\right)\psi\left(\mathbf{k} = (k_i, k_j + d), t\right)\right\rangle \qquad 15$$

$\psi(\mathbf{k})$is the order parameter which equals the composition difference of the two polymers in the element **k**, and d is a positive variable and varies from 1 to k_i. The angle brackets denote the average value of the expression inside the brackets over all the lattice points. The characteristic length in the ith dimension, $R_i(t)$, is the first zero value of $g_i(d, t)$.

The interface of the polymer and the patterned substrate is the focus of this study. For improved model fidelity, the characteristic length is measured by a 2D model of 128×128 elements instead of a 3D model. The phase separation takes place on a neutral substrate and the effect of the elastic field is included. It has been previously established that $R(t)$ increases proportionally to $t^{1/3}$ [14-16]. The value of $R(t)$ is obtained by evaluation of $g_i(d, t)$. $R(t)$ is determined with first order interpolation between the two points when the sign of the pair-correlation function changes, as can be seen in Figure 1.

In Figure 1 the $R(t)$ value without the elastic energy can be fitted to a straight line with the x-axis set to be $t^{1/3}$. The slope of the fitting line is 0.545. The value of $R(t)$ in the system with the consideration of isotropic energy evolves more slower than that in the elasticity free system, as can be observed in Figure 1. In an isotropic elastic system, the $R(t)$ value can also be fitted with a straight line with the respect of $t^{1/3}$, and the slope of the fitting line is 0.370, smaller than

that for the elasticity free situation. This result is due to the elastic free energy term added to the local free energy, which slows the minimization of the free energy.

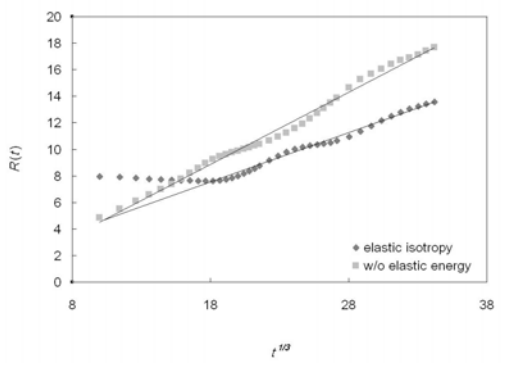

Figure 1 The relationship of the characteristic length, $R(t)$, and the time, t.

To optimize the final pattern according to the functionalized substrate, the characteristic length should be compatible with the pattern scale. The similarity of the final pattern to the pattern on the substrate is measured with respect to time. The compatibility of the final pattern and the patterns designed on the substrate is measured by a factor, C_S

$$C_S = \frac{1}{2}\left\langle \left| \psi(\mathbf{k}) - S_k \right| \right\rangle \qquad 16$$

where

$$S_k = \begin{cases} \dfrac{s_1(k)}{\left|s_1(k)\right|}, & s_1(k) \neq 0 \\ 0, & s_1(k) = 0 \end{cases} \qquad 17$$

$s_1(\mathbf{k})$ is the parameter in the surface energy, which denotes the strength of the surface functionalization. $s_1(\mathbf{k})$ can be varies across the substrate surface. S_k is the qualitative representation of the substrate attraction. Obviously,

$$0 \le C_S \le 1$$

The greater the value of C_S, the more compatible the resulting polymer morphology is to the functionalized substrate. The phase separation is simulated numerically in a 128×128 elements 2D model on a heterogeneously functionalized substrate. Figure 2 shows the value $R(t)$ across the direction perpendicular to the strips patterns on the substrate. It can be seen that $R(t)$ in the x direction increases quickly in the early stage and slows beyond a critical value, which is related to the dimension of the pattern strips. The system with isotropic elastic energy has smaller evolution rates but an earlier critical time than the phase separation without elastic energy. It can be seen that the characteristic length can be fitted into straight lines before and after the critical time, both in the situations with and without elastic energy.

In Figure 3 the compatibility factor, C_S is also plotted with $t^{1/3}$. There is also a critical time during the evolution of the compatibility factors. It can be observed that the critical time for C_S is empirically identical with that of $R(t)$ in Figure 2. The compatibility of the phase separation pattern with the substrate increases quickly before the critical time and become stable afterward. After the critical time, $R(t)$ and C_S increase in a much slower pace. In practice, this implies that the optimized annealing time should be close to the critical time, since a longer annealing time does not help to significantly refine the final pattern.

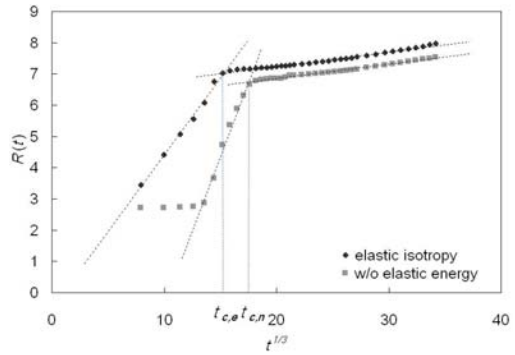

Figure 2 The Characteristic length in x direction (the direction perpendicular to the strips in the pattern)

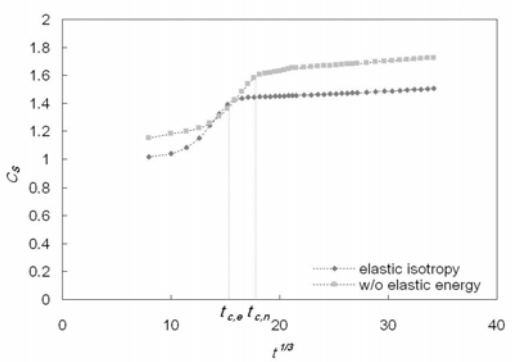

Figure 3 The compatibility of the result pattern to the patterned substrate

The lateral composition profile of phase decomposition with a patterned substrate is observed in a 3D model. A checker board structure is observed in the early stage of the phase separation as reported in other papers [17, 18]. Since the attraction factor is alternating on the substrate, the polymer near the substrate is attracted and attached to the respective area on the substrate, and the neighboring part in the domain to the depth direction is concentrated with the other type of polymer. This effect starts from the interface with the substrate and decays through the thickness direction to the domain. As the spinodal decomposition develops in the bulk domain, the random phase separation overcomes the checker board effect.

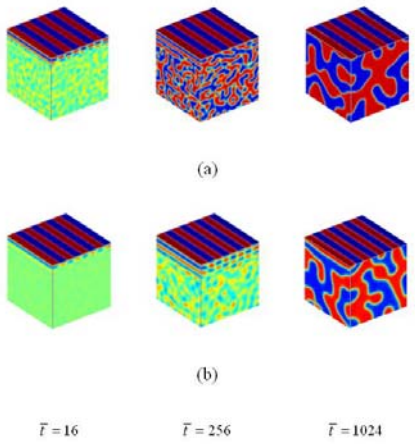

Figure 4 Effect of the heterogeneously functionalized pattern on the phase decomposition. (a) without elastic energy; (b) with isotropic elastic energy.

4 CONCLUSIONS

2D and 3D numerical simulations are developed for the phase separation of a binary immiscible polymer blend. The effect of isotropic elastic energy is investigated. It is observed that in the spinodal decomposition process, the characteristic length, $R(t)$, is proportional to $t^{1/3}$. The involvement of the isotropic elastic energy results in a smaller slope in the $R(t)$~$t^{1/3}$ diagram. The introduction of a patterned substrate with regular strips will induce a critical time in both the $R(t)$ in the direction perpendicular to the strips, and the compatibility of the result pattern and the substrate pattern, C_S. The strips confine the increase of $R(t)$ in the direction perpendicular to the strips. The slope of $R(t)$~$t^{1/3}$ diagram decreases in the second stage.

The lateral composition profile is investigated in a 3D model. A checker board structure is shown in the early stage of the decomposition and decays as the intrinsic value of $R(t)$ in the bulk domain increases.

REFERENCES

[1]. Cahn, J.W. and J.E. Hilliard, *Free Energy of a Nonuniform System. I. Interficial Free Energy.* The Journal of Chemical Physics, 1958. **28**(2): p. 258-267.

[2]. Flory, P.J., *Principles of Polymer Chemistry*. 1953, Ithaca, NY: Cornell University Press.

[3]. L. Vegard, Z., *The constitution of mixed crystals and the space occupied by atoms.* Phys, 1921. **5**(17).

[4]. Denton, A.R. and N.W. Ashcroft, *Vegard's law.* Physical Review A, 1991. **43**(6): p. 3161-3164.

[5]. AG, K., *Theory of structrual transformations in solids*. 1983, New York: Wiley.

[6]. Seol, D.J., et al., *Computer simulation of spinodal spinodal decomposition in constrained films.* Acta Maerialia, 2003. **51**(17): p. 5173-5185.

[7]. Copetti, M.L.M. and C.M. Elliot, *Kinetics of Phase Decomposition Process:Numerical Solutions to Cahn-Hilliard Equation.* Material Science and Technology, 1990. **6**: p. 279-296.

[8]. Eyre, D.J., *An Unconditionally Stable One-step Scheme for Gradient Systems.* Unpublished article, 1998.

[9]. Eyre, D.J., *Unconditionally Gradient Stable Time Marching the Cahn-Hilliard Equation.* Unpublished article, 1998.

[10]. Mauri, R., R. Shinnar, and G. Triantafyllow, *Spinodal decomposition in binary mixtures.* Physical Review E, 1996. **53**(3): p. 2613-2623.

[11]. Kressler, J., et al., *Temperature Dependence of the Interaction Parameter between Polystyrene and Poly(methyl methacrylate).* Macromolecules, 1994. **27**: p. 2448-2453.

[12]. Wise, S.M. and W.C. Johnson, *Numerical Simulations of Pattern-directed Phase Decomposition in a Stressed, Binary Thin Film.* Journal of Applied Physics, 2003. **94**(2): p. 889-898.

[13]. Jones, R.A.L., *Effect of Long-Range Forces on Surface Enrichment in Polymer Blends.* Physics Review E, 1993. **47**(2): p. 1437-1440.

[14]. Brown, G. and A. Chakrabarti, *Surface-directed Spinodal Decomposition in a Two-Dimensional Model.* Physical Review A, 1992. **46**(8): p. 4829-4835.

[15]. Wheeler, A.A., W.J. Boettinger, and G.B. McFadden, *Phase-field Model for Isothermal Phase Transitions in Binary Alloys.* Physics Review A, 1992. **45**(10): p. 7424-7439.

[16]. Jones, R.A.L., L.J. Norton, and E.J. Kramer, *Surface-directed Spinodal Decomposition.* Physical Review Letters, 1991. **66**(10): p. 1326-1329.

[17]. A.Karim, et al., *Phase Separation of Ultrathin Polymer-blend Films on Patterned Substrates.* Physical Review E, 1998. **57**(6): p. 6273-6276.

[18]. Kielhorn, L. and M. Muthukumar, *Phase Separation of Polymer Blend Film near Patterned Surfaces.* Journal of Chemical Physics, 1999. **111**(5): p. 2259-2269.